

## Cerium filling and doping of cobalt triantimonide

Donald T. Morelli and Gregory P. Meisner

*Physics and Physical Chemistry Department, General Motors Research and Development Center, Warren, Michigan 48090*

Baoxing Chen, Siqing Hu, and Ctirad Uher

*Department of Physics, University of Michigan, Ann Arbor, Michigan 48109*

(Received 20 May 1997)

We have fabricated and studied the structural, magnetic, and transport properties of filled skutterudites of the form  $Ce_yFe_{4-x}Co_xSb_{12}$  with  $0 < y < 1$  and  $x = 3.25$  and  $4$ . For samples containing 100% Co, Ce can be inserted into approximately 10% of the voids in the skutterudite structure. It is shown that the rare earth is trivalent and dopes the host  $CoSb_3$   $n$ -type. With substitution of Fe for Co the void occupancy by Ce increases. The thermal conductivity is strongly depressed even at small (5%) rare-earth filling fractions, and is further degraded by substitution of Fe for Co. Although the electron mobility in  $n$ -type samples is smaller than the hole mobility in  $p$ -type samples, due to their large electron masses the Seebeck coefficient in  $n$ -type material maintains large values at high electron concentrations. [S0163-1829(97)02036-5]

### INTRODUCTION

The recent discovery of high thermoelectric figure of merit in certain skutterudite compounds<sup>1,2</sup> has opened up the possibility of fabricating highly efficient thermoelectric generators for the conversion of waste heat to electricity. The operation of such generators requires the use of both  $n$ - and  $p$ -type thermoelectric materials. Up to now the materials in this family that have been reported upon exhibit  $p$ -type behavior only. Recently, Chen *et al.*<sup>3</sup> predicted that in the filled skutterudite  $CeFe_{4-x}Co_xSb_{12}$   $n$ -type material should be obtained for  $x \approx 3$ . From band-structure calculations, Nördstrom and Singh<sup>4</sup> showed that  $n$ -type materials should have large electron masses that could lead to desirable thermoelectric properties. In this paper we will describe the results of our studies of the structural, magnetic, and low-temperature transport properties of such  $n$ -type skutterudite compounds.

The thermoelectric figure of merit of a material is given by  $Z = S^2\sigma/\kappa$ , where  $S$  is the Seebeck coefficient,  $\sigma$  the electrical conductivity, and  $\kappa$  the thermal conductivity. Since the dimensions of  $Z$  are inverse temperature, it is customary to define the dimensionless figure of merit  $ZT$ , where  $T$  is the absolute temperature. The observation of thermoelectric figure of merit in  $p$ -type  $LaFe_{4-x}Co_xSb_{12}$  (Ref. 1,  $ZT = 0.9$  at 800 K) and  $CeFe_{4-x}Co_xSb_{12}$  (Ref. 1,  $ZT = 0.7$  at 800 K; Ref. 2,  $ZT = 1.2$ – $1.4$  at 900 K) filled skutterudite compounds as good as or better than state-of-the-art thermoelectric materials ( $ZT \leq 1$ ) is the latest step in the study and optimization of the thermoelectric properties of these fascinating materials. These filled skutterudites are derived from binary (unfilled) skutterudites of the form  $AB_3$ , where  $A$  is Co, Rh, or Ir and  $B$  is P, As, or Sb. The structure of these materials has been well determined experimentally<sup>5-7</sup> and consists of a cubic array of metal  $A$  atoms containing four-membered square planar rings of pnictide  $B$  atoms. The potential of the binary compounds as  $p$ -type thermoelectric materials was first suggested by Fleurial, Caillat, and Borshchevsky<sup>8</sup> based on their observation of the combination of high hole mobility and

potentially small lattice thermal conductivity due to the complex crystal structure (16 atoms per unit cell) and heavy atom masses. Indeed, subsequent study of the thermoelectric properties of  $CoSb_3$  and  $IrSb_3$  showed that the power factor (the numerator  $S^2\sigma$  entering into the figure of merit) is quite large and comparable to that of state-of-the-art thermoelectric materials such as  $Bi_2Te_3$  and  $PbTe$ . Singh and Pickett<sup>9</sup> carried out band-structure calculations for these materials and showed that the skutterudites are very narrow or zero-band-gap semiconductors characterized by a linearly dispersing valence band and conduction bands of large effective mass. The observed transport properties of  $p$ -type single crystals of  $CoSb_3$  (Ref. 10) were consistent with this valence-band picture. Unfortunately, although the power factor for binary skutterudites is large, the thermal conductivity, while moderately small, is about a factor 10 too high to make these compounds useful as thermoelectrics. Borshchevsky, Caillat, and Fleurial<sup>11</sup> showed that it is possible to make mixed crystals of skutterudites that exhibit lower lattice thermal conductivity due to alloy scattering; however, this technique raises the figure of merit up to only about half that of state-of-the-art materials.

Interest in the use of these compounds as thermoelectric materials most likely would have ceased at this point were it not for the observation of Slack and Tsoukala<sup>12</sup> that the skutterudite structure is amenable to modification in the direction of a greatly reduced lattice thermal conductivity. They pointed out that skutterudites have large voids which can be "filled" by rare-earth atoms. Such filled skutterudites, which form with Fe, Ru, or Os on the metal site, have been known for some time<sup>13-15</sup> and exhibit a wide range of interesting physical properties, including superconductivity [ $LaFe_4P_{12}$  (Ref. 16)] and hybridization gap semiconducting behavior [ $CeFe_4P_{12}$  (Ref. 17)]. Because the radius of the rare-earth atom is significantly smaller than the radius of the void, the former "rattles," i.e., exhibits a soft phonon mode. Experimental evidence of such rattling had already been exhibited in the large x-ray thermal parameter<sup>13-15</sup> characteristic of rare-earth atoms in this structure. Recently, Morelli and

TABLE I. Nominal overall compositions, composition of the skutterudite phase, and presence of secondary phases in  $Ce_yFe_{4-x}Co_xSb_{12}$  samples; the designation ‘‘S’’ indicates those samples which are saturated with Ce as determined from analysis of the x-ray spectra and susceptibility.

Sample number and nominal composition	Composition of the skutterudite phase	Secondary phases
1:CoSb <sub>3</sub>		
2:Ce <sub>0.050</sub> Co <sub>4</sub> Sb <sub>12</sub>	Ce <sub>0.044</sub> Co <sub>4</sub> Sb <sub>11.62</sub>	none
3:Ce <sub>0.075</sub> Co <sub>4</sub> Sb <sub>12</sub>	Ce <sub>0.072</sub> Co <sub>4</sub> Sb <sub>11.62</sub>	none
4:Ce <sub>0.100</sub> Co <sub>4</sub> Sb <sub>12</sub>	Ce <sub>0.085</sub> Co <sub>4</sub> Sb <sub>12</sub>	none
5:Ce <sub>0.150</sub> Co <sub>4</sub> Sb <sub>12</sub> (S)	Ce <sub>0.100</sub> Co <sub>4</sub> Sb <sub>11.53</sub>	CeSb <sub>2</sub> (<1%)
6:Ce <sub>0.200</sub> Co <sub>4</sub> Sb <sub>12</sub> (S)	Ce <sub>0.089</sub> Co <sub>4</sub> Sb <sub>11.47</sub>	CeSb <sub>2</sub> (<5%)
7:Ce <sub>0.2</sub> Fe <sub>0.75</sub> Co <sub>3.25</sub> Sb <sub>12</sub>		
8:Ce <sub>0.3</sub> Fe <sub>0.75</sub> Co <sub>3.25</sub> Sb <sub>12</sub>		
9:Ce <sub>0.5</sub> Fe <sub>0.75</sub> Co <sub>3.25</sub> Sb <sub>12</sub> (S)	Ce <sub>0.22</sub> Fe <sub>0.63</sub> Co <sub>3.37</sub> Sb <sub>11.47</sub>	CeSb <sub>2</sub> (<10%) (Fe,Co)Sb <sub>2</sub> (<5%)
10:Ce <sub>1</sub> Fe <sub>0.75</sub> Co <sub>3.25</sub> Sb <sub>12</sub> (S)	Ce <sub>0.31</sub> Fe <sub>0.75</sub> Co <sub>3.25</sub> Sb <sub>11.47</sub>	CeSb <sub>2</sub> (<20%) (Fe,Co)Sb <sub>2</sub> (<5%)

Meisner<sup>18</sup> provided experimental evidence of the reduction in lattice thermal conductivity relative to unfilled skutterudites for CeFe<sub>4</sub>Sb<sub>12</sub>. These results were confirmed shortly thereafter on various rare-earth filled skutterudites by Nolas *et al.*<sup>19</sup>

While void filling thus can produce a strong reduction in the lattice thermal conductivity of skutterudites, the introduction of a primarily trivalent rare-earth ion influences the electronic structure and transport properties. Indeed, in CeFe<sub>4</sub>Sb<sub>12</sub>, from a purely crystal chemistry point of view, the substitution of Fe for Co provides four additional holes in the valence band, only three of which are filled by electrons from the rare earth; there is thus one additional hole per formula unit, and this material should be a *p*-type semimetal, in agreement with experiment.<sup>18</sup> The studies of Sales, Mandrus, and Williams<sup>1</sup> and Fleurial *et al.*<sup>2</sup> showed that by partial substitution of Co on the Fe site, the hole concentration decreases, causing an increase in the Seebeck coefficient that then gives rise to the enhanced thermoelectric properties. It was perhaps surprising that one can partially substitute Co for Fe in CeFe<sub>4</sub>Sb<sub>12</sub> (and related) filled skutterudites since it was previously thought that such compounds would not form with Co on the transition-metal site. We recently<sup>3</sup> carried out a detailed study of Ce<sub>y</sub>Fe<sub>4-x</sub>Co<sub>x</sub>Sb<sub>12</sub> with  $0 < x < 2$  and showed that the amount of Ce in the voids, *y*, decreases strongly with Co substitution, and the resultant transport and thermoelectric properties are determined by the subtle interplay between Co doping *x* on the Fe site and the rare-earth filling parameter *y*. On the basis of these results, it was suggested that a crossover to *n*-type behavior would occur for  $x \approx 3$ . In addition to the fascinating electronic properties of Ce<sub>y</sub>Fe<sub>4-x</sub>Co<sub>x</sub>Sb<sub>12</sub>, the *thermoelectronic* properties are further influenced by the effect of Co doping and rare-earth atom filling fraction on the lattice thermal conductivity. In the present investigation we explore further the (*x*,*y*) phase space in the region where crossover of the carrier type is expected to occur in order to produce *n*-type material and to study the individual influence of *x* and *y* on the various transport properties.

## EXPERIMENTAL DETAILS

Samples of Ce<sub>y</sub>Fe<sub>4-x</sub>Co<sub>x</sub>Sb<sub>12</sub> with  $x=4.00$  (samples 1–6) and  $x=3.25$  (samples 7–10) were prepared with various Ce filling fractions *y* using the method described in Ref. 3. Table I shows the starting compositions determined from the mass of the constituent elements prior to synthesis. The structure, phase, and composition were also characterized using x-ray diffraction and microprobe analysis, the results of which will be described in detail below.

Magnetic-susceptibility measurements were carried out using a Quantum Design superconducting quantum interference device (SQUID) susceptometer on portions of these samples with typical masses of a few hundred milligrams. The samples were placed inside a polyethylene capsule and straw, the diamagnetic signal of which was first measured and corrected for. Electrical and thermal transport property measurements were carried out using the methods described in detail previously.<sup>3</sup>

## RESULTS AND DISCUSSION

### A. Structure

Figure 1 displays typical x-ray diffraction results on several samples containing 100% Co. All samples display peaks characteristic of the filled skutterudite structure from which lattice constants can be derived. In addition, we see that for samples containing higher concentrations of Ce there appear additional small peaks which we attribute to an impurity phase.

A plot of lattice constant versus Ce concentration (Fig. 2) for the two series of samples with  $x=3.25$  and  $4.00$  reveals that the lattice constant increases in proportion to the amount of Ce in the sample up to a point which moves outward in Ce concentration with a decrease in Co content. This indicates that at low concentrations the Ce is incorporated into the void in the skutterudite structure but that at some point, dependent on the Co (or Fe) content, the void filling becomes saturated and any additional Ce above this limit is presumably incorporated into the impurity phase which appears in

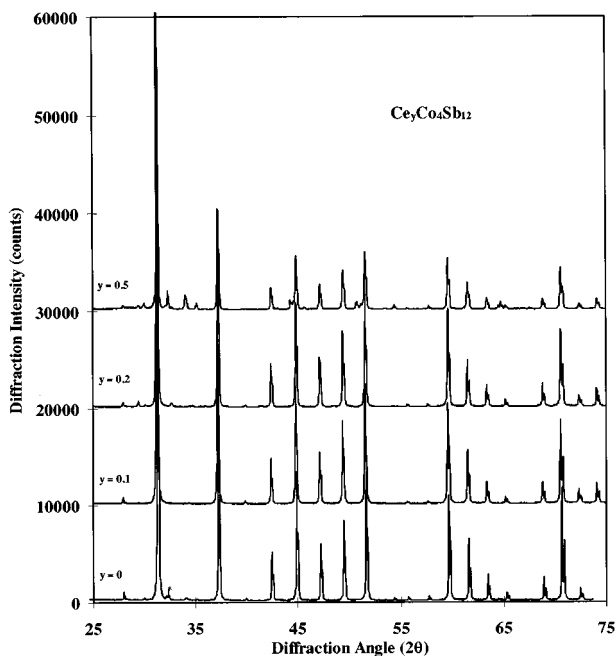


FIG. 1. Typical x-ray diffraction patterns for  $\text{Ce}_y\text{Co}_4\text{Sb}_{12}$  samples. A small amount of  $\text{CoSb}_2$  in the  $y=0$  sample is indicated by the asterisk (\*). The  $y=0.1$  sample contains no significant amount of impurity phases whereas the  $y=0.2$  and  $0.5$  show increasing amounts of impurity phases.

the x-ray diffraction patterns, such as those for  $\text{Ce}_{0.2}\text{Co}_4\text{Sb}_{12}$  and  $\text{Ce}_{0.5}\text{Co}_4\text{Sb}_{12}$  in Fig. 1. Samples for which this limit has been surpassed are saturated with Ce and are designated with an “S” in Table I. Thus for samples containing no Fe, i.e., pure  $\text{Co}_4\text{Sb}_{12}$ , Ce can be incorporated in the void up to about 10% filling fraction, while for an Fe/Co ratio of 0.75/3.25, (i.e., about 23% Fe) about 30% of the voids can be filled with Ce. This is consistent with our previous results<sup>3</sup> that showed that for samples containing all Fe ( $\text{CeFe}_4\text{Sb}_{12}$ ) nearly all of the voids are filled while for non-Fe containing samples the filling fraction was determined to be about 7%.

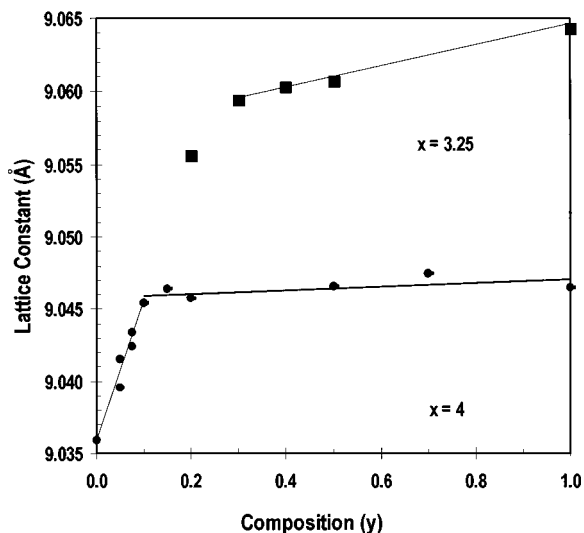


FIG. 2. Lattice constants of  $\text{Ce}_y\text{Fe}_{4-x}\text{Co}_x\text{Sb}_{12}$  as a function of Ce concentration  $y$  for samples with Co concentrations of  $x=4$  and  $3.25$ .

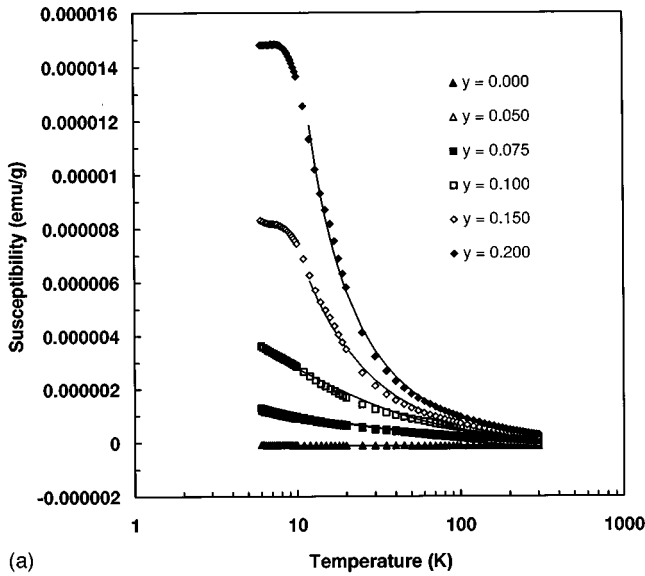
In order to gain more information about the phase and composition of these samples, we performed microprobe analysis on a selection of the samples, the results of which are given in Table I. For the samples containing 100% Co, a single phase skutterudite compound is obtained up to a Ce content  $y=0.1$ . For  $y=0.15$  and  $0.2$ , we see no increase in the amount of Ce incorporated in the void but rather the formation of a secondary phase which has been identified as  $\text{CeSb}_2$ . This is the phase which gives rise to the impurity peaks in the x-ray diffraction patterns for the saturated samples in Fig. 1. For the Fe-containing samples above the saturation limit, again the amount of Ce in the void in the skutterudite structure is less than the overall Ce composition and the formation of a secondary phase occurs, in complete agreement with the x-ray diffraction data.

### B. Magnetic susceptibility

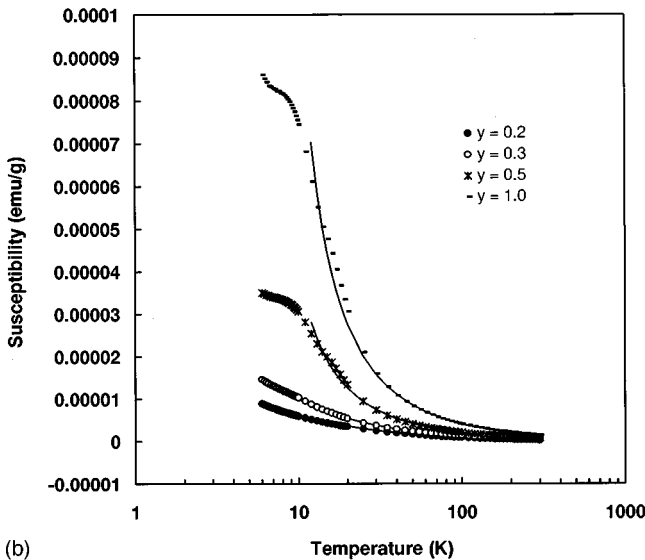
In the unfilled skutterudite  $\text{CoSb}_3$  the bonding is such that three electrons from each Co atom participate in bonding with Sb via hybridized  $d^2s$  orbitals. The remaining six non-bonding  $d$  electrons of Co are paired together in three  $d$  orbitals in a nonmagnetic  $d^6$  state; thus this compound is diamagnetic.<sup>20</sup> Danebrock, Evers, and Jeitschko<sup>21</sup> have recently measured the susceptibility of filled skutterudites containing 100% Fe on the transition-metal site ( $x=0$ ) and concluded that Fe has a nonzero moment in these compounds. From magnetic susceptibility and Mössbauer studies on filled skutterudite phosphides, on the other hand, Grandjean *et al.*<sup>22</sup> concluded that the Fe in these compounds is in the nonmagnetic  $d^6$  ( $\text{Fe}^{2+}$ ) state. The charge state of Fe in  $\text{CeFe}_{4-x}\text{Co}_x\text{Sb}_{12}$  is of significance because it can potentially influence the nature of the electrical and thermal transport properties. Figure 3(a) shows the susceptibility for the samples containing 100% Co (nos. 1–6) from 6–300 K. As expected,  $\text{CoSb}_3$  is diamagnetic while a Curie-like behavior develops in samples containing Ce. Figure 3(b) shows similar behavior for the Fe-containing samples nos. 7–10. A somewhat different perspective on the susceptibility can be gained by plotting  $\chi T$  versus  $T$ ; see Fig. 4. In this plot we see a direct correlation between samples which are saturated with Ce (nos. 5, 6, 9, and 10) and the occurrence of a peak in  $\chi T$  at low temperatures. This peak in  $\chi T$  corresponds to a kink in the susceptibility curves in Fig. 3. We thus attribute this feature to the formation of  $\text{CeSb}_2$  in these samples which was observed in the x-ray diffraction and microprobe analysis results described above. We have fit the susceptibility data below 100 K to a Curie law

$$\chi = C/(T + \theta) + \chi_0, \quad (1)$$

where  $C$  is the Curie constant,  $\theta$  the Curie-Weiss temperature, and  $\chi_0$  the background susceptibility. For saturated samples this fit was terminated at 10 K in order to minimize the effect of the  $\text{CeSb}_2$  impurity phase. The results of this fitting procedure are tabulated in Table II and shown by the solid lines in Figs. 3(a) and 3(b). Figure 5 is a plot of the Curie constant  $C$  as a function of overall Ce concentration for all of these samples. It is quite clear from this plot that Ce in the filled skutterudite structure studied here, possessing an average effective moment of 2.36 Bohr magnetons, is in the trivalent state, experimentally confirming the prediction of



(a)



(b)

FIG. 3. (a) Magnetic susceptibility of  $Ce_yCo_4Sb_{12}$  for various Ce filling fractions. Solid lines are fits to the Curie-Weiss law  $\chi = C(T + \theta) + \chi_0$  with parameters given in Table II. (b) Magnetic susceptibility of  $Ce_yFe_{0.75}Co_4Sb_{12}$  for various Ce filling fractions. Solid lines are fits to the Curie-Weiss law  $\chi = C(T + \theta) + \chi_0$  with parameters given in Table II.

Nördstrom and Singh;<sup>4</sup> it is an important factor to keep in mind in interpreting the electrical transport properties. Moreover, we see no enhancement of the local moment in samples containing Fe, implying that the electronic configuration of the Fe, at least in the concentration range studied here, must be the  $Fe^{2+}$  (zero spin  $d^6$ ) state, as in the phosphides, which, as we shall see below, is consistent with the observed electronic properties.

### C. Electrical resistivity, Hall coefficient, and Seebeck coefficient

Our nominally undoped sample of  $CoSb_3$  (no. 1) is  $n$ -type and possesses a resistivity of approximately  $0.1 \Omega \text{ cm}$  at room temperature. The observation of  $n$ -type behavior in pure  $CoSb_3$  is somewhat unusual as in most cases  $p$ -type

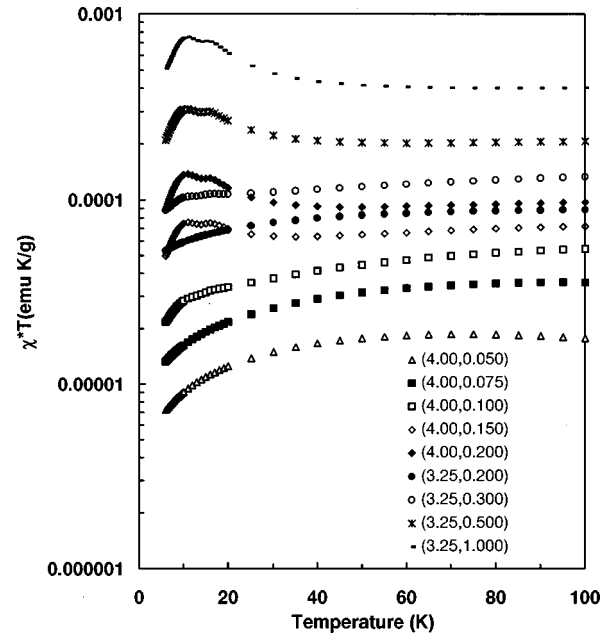


FIG. 4. The product of susceptibility times temperature  $\chi T$  as a function of temperature for various  $(x,y)$  combinations of  $Ce_yFe_{4-x}Co_xSb_{12}$ .

behavior is observed, and requires some discussion. The carrier type one obtains in pure  $CoSb_3$  depends on whether the samples are grown under Sb-rich or Sb-deficient conditions. Samples grown under Sb-rich conditions will be  $p$ -type<sup>8,23</sup> as this corresponds to an absence of a Co atom that leads to the formation of holes in the valence band. As can be seen from Table I, our samples are all Sb deficient, which leads to an excess of electrons in the conduction band and  $n$ -type behavior. The crossover from  $p$ -type to  $n$ -type behavior in  $CoSb_3$  as one proceeds from an Sb-rich to an Sb-deficient condition was first noted by Dudkin and Abrikosov;<sup>24</sup> Sharp *et al.*<sup>25</sup> observed a crossover from  $p$ -type to  $n$ -type behavior in  $CoSb_3$  after hot pressing that they attributed to a change from an Sb-rich to an Sb-deficient state. It thus appears likely that the heretofore unexplained  $p$ -type behavior and a gradient in hole concentration along the boule in single crystals of skutterudites grown from Sb-rich melts, has its origin in the existence of vacancies on the Co site, whereas an  $n$ -type behavior such as that observed here arises from vacancies on the Sb site.

Figure 6(a) shows the electrical resistivity as a function of temperature for samples containing 100% Co and various Ce filling fractions (nos. 2–6). All are  $n$ -type with electron concentrations and mobilities shown in Table III. The electrical resistivity as a function of temperature for the Fe-containing samples nos. 7–10 (together with the saturated  $Ce_{0.2}Co_4Sb_{12}$  sample no. 6 for comparison) is shown in Fig. 6(b). What appears to be a complex dependence of resistivity on Ce concentration and Co/Fe ratio arises from a subtle interplay between the hole doping by Fe on the Co site and the “doping” by electrons which occurs with the addition of Ce. We have previously suggested<sup>3</sup> that the carrier concentration per formula unit of  $Ce_yFe_{4-x}Co_xSb_{12}$  on the basis of crystal chemistry arguments should be given approximately by  $(p,n) = 4 - x - 3y$ . When this quantity is positive the samples will be  $p$ -type and when it is negative they will be

TABLE II. Susceptibility parameters in  $Ce_yFe_{4-x}Co_xSb_{12}$  samples.

Sample number and nominal composition	Curie constant $C$ (emu K) $g^{-1}$	Background susceptibility $\chi_0$ (emu $g^{-1}$ )	Curie-Weiss temperature $\theta$ (K)
1:CoSb <sub>3</sub>	$5.00 \times 10^{-7}$	$-1.23 \times 10^{-7}$	4.3
2:Ce <sub>0.050</sub> Co <sub>4</sub> Sb <sub>12</sub>	$4.31 \times 10^{-5}$	$-1.57 \times 10^{-7}$	30.2
3:Ce <sub>0.075</sub> Co <sub>4</sub> Sb <sub>12</sub>	$3.15 \times 10^{-5}$	$-3.64 \times 10^{-8}$	20.2
4:Ce <sub>0.100</sub> Co <sub>4</sub> Sb <sub>12</sub>	$5.77 \times 10^{-5}$	$-2.00 \times 10^{-8}$	10.6
5:Ce <sub>0.150</sub> Co <sub>4</sub> Sb <sub>12</sub> (S)	$8.98 \times 10^{-5}$	$-7.98 \times 10^{-8}$	12.4
6:Ce <sub>0.200</sub> Co <sub>4</sub> Sb <sub>12</sub> (S)	$9.87 \times 10^{-5}$	$-1.47 \times 10^{-8}$	1.2
7:Ce <sub>0.2</sub> Fe <sub>0.75</sub> Co <sub>3.25</sub> Sb <sub>12</sub> (S)	$9.19 \times 10^{-5}$	$-2.70 \times 10^{-8}$	5.2
8:Ce <sub>0.3</sub> Fe <sub>0.75</sub> Co <sub>3.25</sub> Sb <sub>12</sub> (S)	$1.13 \times 10^{-4}$	$2.13 \times 10^{-7}$	1.6
9:Ce <sub>0.5</sub> Fe <sub>0.75</sub> Co <sub>3.25</sub> Sb <sub>12</sub> (S)	$1.74 \times 10^{-4}$	$2.13 \times 10^{-7}$	-5.73
10:Ce <sub>1</sub> Fe <sub>0.75</sub> Co <sub>3.25</sub> Sb <sub>12</sub> (S)	$3.38 \times 10^{-4}$	$3.14 \times 10^{-7}$	-8.25

*n*-type. This scenario is consistent with the  $Fe^{2+}$  state inferred from the susceptibility. This trend in carrier concentration is indeed followed in these samples; for example, sample no. 7 with  $x=3.25$  and  $y=0.2$  is *p*-type while no. 8 with  $x=3.25$  and  $y=0.3$  is *n*-type. The measured hole (or electron) concentrations as determined by our Hall measurements are given in Table III. The mobility for samples containing Fe is significantly smaller than that in samples 1–6 containing all Co, implying that there is significant carrier scattering on the Fe site, a factor which will be important in optimizing the thermoelectric properties of these compounds. In addition, within the series of Fe-containing samples, the hole mobility is larger than the electron mobility due to the difference between valence- and conduction-band masses,<sup>9</sup> a feature characteristic of skutterudite compounds in general. This factor also explains the qualitatively different positive temperature coefficient of resistivity for the *p*-type sample, since the mobility is still increasing at low temperature whereas for the *n*-type samples it is roughly constant or decreases at low temperature.

The Seebeck coefficient of samples 2–6 is displayed in Fig. 7(a) and shows only a weak dependence on electron

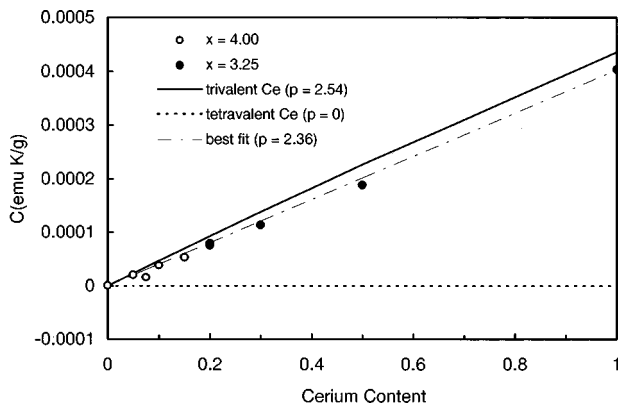


FIG. 5. Curie constant as a function of Ce concentration  $y$  in  $Ce_yFe_{4-x}Co_xSb_{12}$ . Open circles,  $x=4.00$ ; closed circles,  $x=3.25$ . Solid line, theoretical Curie constant for trivalent Ce, corresponding to an effective moment per Ce atom of 2.54 Bohr magnetons; dashed line, Curie constant = 0 (tetravalent Ce); chain line, best fit through the data yielding an effective moment per Ce atom of 2.36 Bohr magnetons.

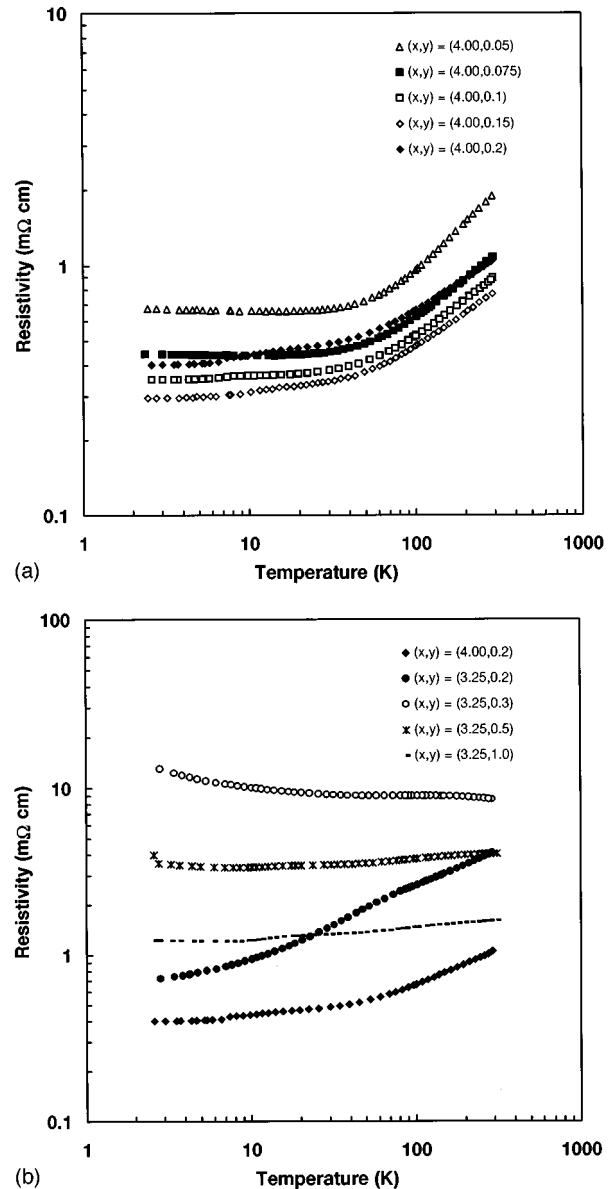


FIG. 6. (a) Resistivity as a function of temperature for  $Ce_yCo_4Sb_{12}$ . (b) Resistivity as a function of temperature for  $Ce_yFe_{4-x}Co_xSb_{12}$ .

TABLE III. Some room-temperature electrical transport properties of  $\text{Ce}_y\text{Fe}_{4-x}\text{Co}_x\text{Sb}_{12}$  samples.

Nominal composition	Measured carrier density ( $\text{cm}^{-3}$ ) and type	Hall mobility ( $\text{cm}^2 \text{V}^{-1} \text{s}^{-1}$ )	Electron mass $m^*$
$\text{CoSb}_3$	$6.1 \times 10^{17} e$	72	
$\text{Ce}_{0.050}\text{Co}_4\text{Sb}_{12}$	$6.0 \times 10^{19} e$	55	1.83
$\text{Ce}_{0.075}\text{Co}_4\text{Sb}_{12}$	$1.4 \times 10^{20} e$	41	2.4
$\text{Ce}_{0.100}\text{Co}_4\text{Sb}_{12}$	$2.8 \times 10^{20} e$	25	4.3
$\text{Ce}_{0.150}\text{Co}_4\text{Sb}_{12}$	$2.4 \times 10^{20} e$	34	
$\text{Ce}_{0.200}\text{Co}_4\text{Sb}_{12}$	$3.2 \times 10^{20} e$	19	
$\text{Ce}_{0.2}\text{Fe}_{0.75}\text{Co}_{3.25}\text{Sb}_{12}$	$2.7 \times 10^{19} h$	71	
$\text{Ce}_{0.3}\text{Fe}_{0.75}\text{Co}_{3.25}\text{Sb}_{12}$	$4.8 \times 10^{20} e$	1.57	6.1
$\text{Ce}_{0.5}\text{Fe}_{0.75}\text{Co}_{3.25}\text{Sb}_{12}$	$2.6 \times 10^{21} e$	0.79	
$\text{Ce}_1\text{Fe}_{0.75}\text{Co}_{3.25}\text{Sb}_{12}$	$8.2 \times 10^{21} e$	0.72	

concentration. The Seebeck coefficient of the undoped sample no. 1 is approximately  $-650 \mu\text{V}/\text{K}$ , consistent with its high resistivity. Figure 7(b) shows results for the Fe-containing samples 7–10 (again including sample 6 for comparison). Again we observe a weak dependence of  $S$  on electron concentration and a change to a positive value for the single  $p$ -type sample. For this sample we observe a hump in the  $S(T)$  curve near 50 K which we have reported upon earlier.<sup>18</sup> The very large values of the Seebeck coefficient that we observe in  $n$ -type samples are similar to those observed in  $\text{CoSb}_3$  doped with Te or Pd (Ref. 23) and are presumably due to the large electron effective mass. We can gain an estimate of the electron effective mass  $m^*$  using a single parabolic band and the room-temperature Seebeck coefficient and electron concentration values. Assuming acoustic-phonon scattering, in this model the Seebeck coefficient  $S$  and electron concentration  $n$  can be expressed as<sup>26</sup>

$$S = \pm \frac{k_B}{e} \left( \frac{2F_1(\eta)}{F_0(\eta)} - \eta \right) \quad (2)$$

and

$$n = \frac{4}{\sqrt{\pi}} \left( \frac{2\pi m^* k_B T}{h^2} \right)^{3/2} F_{1/2}(\eta), \quad (3)$$

where  $F_i$  are Fermi integrals and  $\eta = E_F/k_B T$ . Here  $E_F$  is the electron Fermi level measured upward from the conduction-band edge. One first calculates the Fermi levels from Eq. (2) and uses this value to determine  $m^*$  from Eq. (3) and the measured electron concentration. We will constrain this procedure to the four  $n$ -type samples which are not saturated with Ce to avoid any complication due to a small secondary phase. Also we do not derive a value for the undoped sample no. 1 since in this case the Seebeck coefficient is not a monotonic function of temperature and thus may be influenced by more than one conduction band. The resultant effective masses for samples 2, 3, 4, and 8 are given in Table III. Since the Ce concentration in these samples is quite low, the Ce atom wave functions will not overlap; the band structure of these samples is thus most likely that of  $\text{CoSb}_3$  doped  $n$ -type by Ce. Figure 8 is a plot of the electron mass as a function of electron concentration in these samples as well as those doped with Te and Pd.<sup>23</sup> We see that the electron masses of these Ce-doped samples are consistent

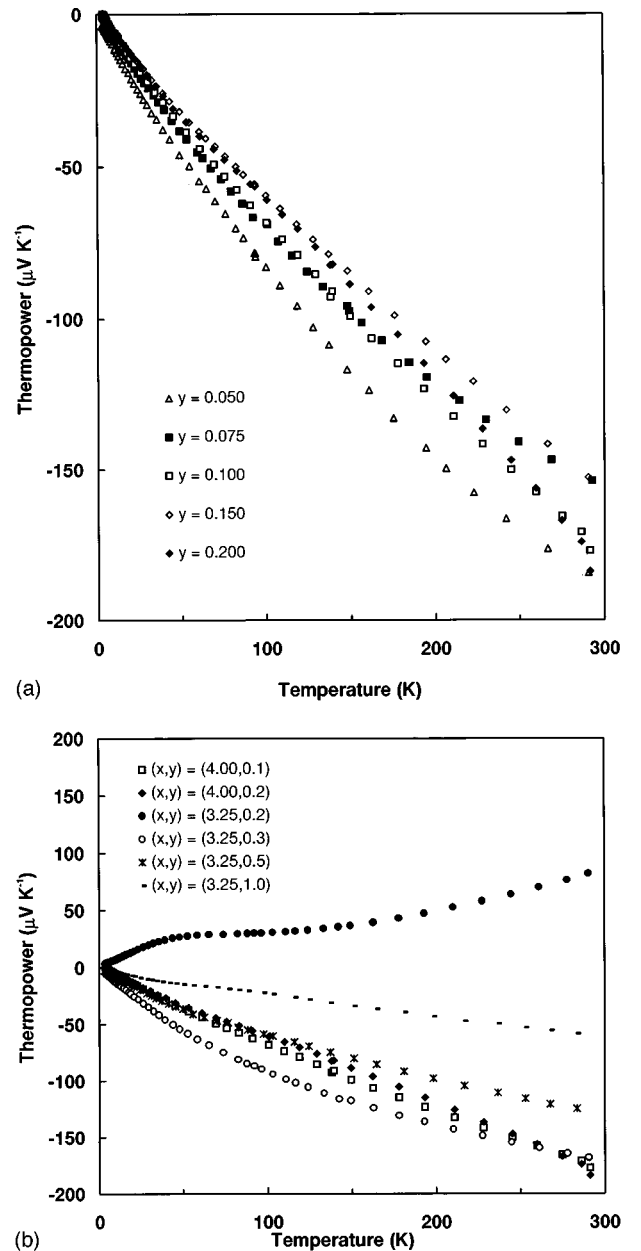


FIG. 7. Thermoelectric power for  $\text{Ce}_y\text{Co}_4\text{Sb}_{12}$  for various Ce filling fractions  $y$ . (b) Thermoelectric power for  $\text{Ce}_y\text{Fe}_{4-x}\text{Co}_x\text{Sb}_{12}$  for various filling fractions  $y$ .

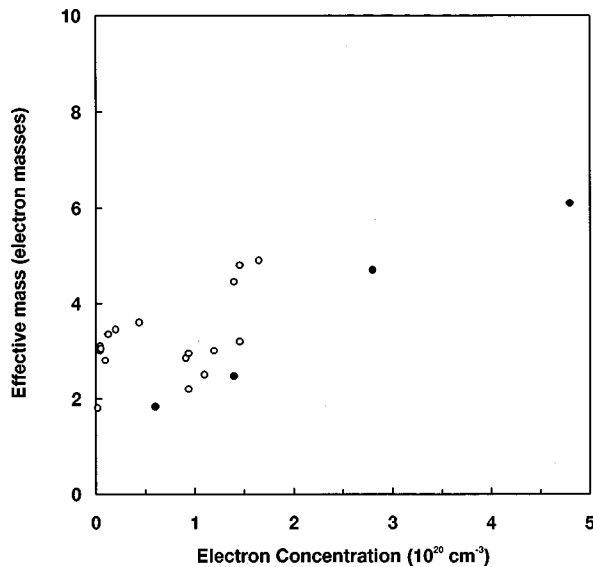


FIG. 8. Electron effective mass as a function of electron concentration in  $n$ -type  $\text{CoSb}_3$ . Open circles, samples doped with Te and Pd (Ref. 23); solid circles, samples filled and doped with Ce.

with Te- and Pd-doped  $n$ -type  $\text{CoSb}_3$  samples and serve to identify Ce as a true  $n$ -type dopant. The large values of  $m^*$  observed here verify band structure calculations which predict a heavy conduction-band mass in this compound.<sup>9</sup>

#### D. Thermal conductivity

Figure 9(a) shows the lattice thermal conductivity  $\kappa$  as a function of temperature for samples nos. 1–6 containing 100% Co. The electronic contribution, which is not more than 25% for any sample, has been subtracted off using the Wiedemann-Franz law. The addition of Ce dramatically reduces the thermal conductivity relative to  $\text{CoSb}_3$ , with the low-temperature peak first being moderately ( $y=0.05$ ) and then strongly diminished ( $y=0.075$  and above). The weak temperature dependence is characteristic of the scattering due to the “rattling” rare-earth atom as has been discussed in detail previously.<sup>19</sup> The present results show that in fact very little Ce is required in order to produce a strong scattering effect. This is similar to the situation in other crystalline materials exhibiting low-frequency phonon modes,  $\text{KBr-KCN}$  mixed crystals being a prime example.<sup>27</sup> Looking now at the Fe-containing samples, Fig. 9(b), we see an additional 50% reduction in  $\kappa$  relative to the non-Fe containing samples. In this series of samples, as the Ce concentration is increased, what remains of the low-temperature peak is depressed further and eventually vanishes, while the room-temperature thermal conductivity is almost independent of Ce concentration, most of the scattering in this temperature range being due to the Fe. This is somewhat surprising since Fe and Co have nearly the same mass and atom size. The origin of the additional strong phonon scattering upon substitution of Fe for Co is not known at this time, but may be related to the valence state of Fe in these compounds, a process which has been suggested to occur in other mixed valence skutterudites.<sup>28,29</sup> The zero-spin  $\text{Fe}^{2+} d^6$  configuration inferred from the magnetic susceptibility is known to be a

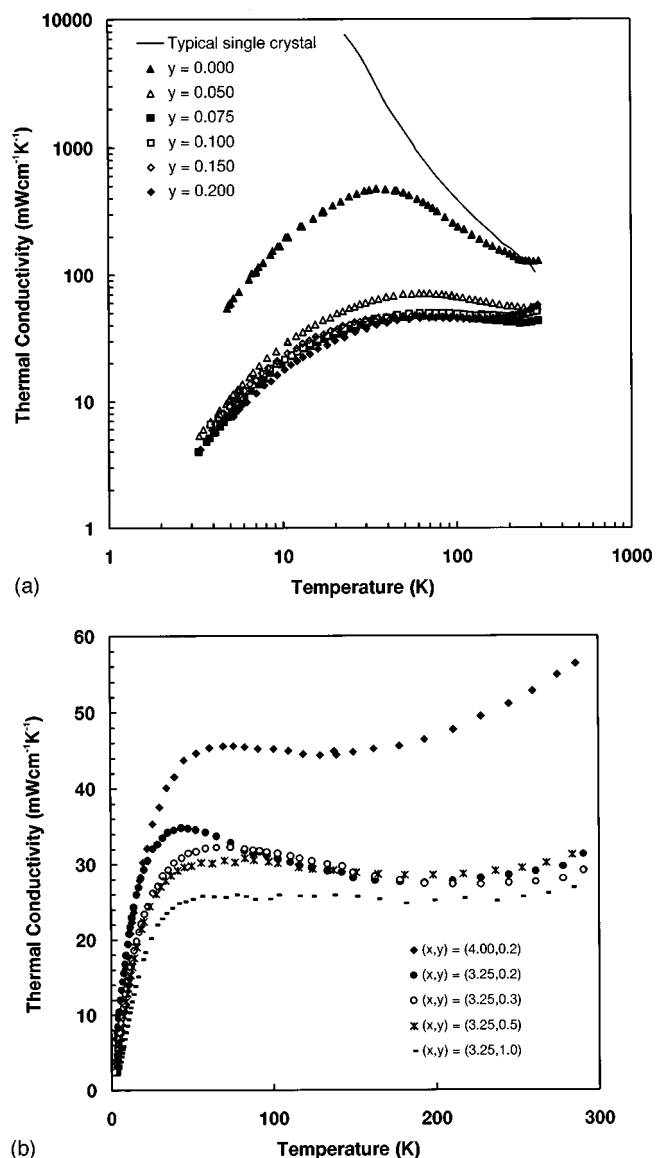


FIG. 9. (a) Thermal conductivity of  $\text{Ce}_y\text{Co}_4\text{Sb}_{12}$  for various Ce filling fractions  $y$ . Solid line represents typical results for single crystal  $\text{CoSb}_3$  (Ref. 8). (b) Thermal conductivity as a function of temperature for  $\text{Ce}_y\text{Fe}_{4-x}\text{Co}_x\text{Sb}_{12}$ .

somewhat energetically unstable one in similar materials such as  $\text{FeS}_2$ . One possible scenario is that a passing phonon could be absorbed and cause a dynamic exchange of electrons between  $\text{Fe}^{2+}$  and  $\text{Co}^{3+}$ , although this seems unlikely given the relative stability of the latter. The interesting effect of Fe substitution on the thermal conductivity deserves further experimental and theoretical scrutiny and will be a subject of future study.

#### E. Thermoelectric figure of merit

From the room-temperature values of Seebeck coefficient, electrical resistivity, and thermal conductivity, we derive the values of dimensionless figure of merit  $ZT = S^2\sigma T/\kappa$ . For samples 7–10 containing Fe, the decrease in thermal conductivity is offset by an increase in electrical resistivity due to scattering on the Fe site, and  $ZT$  does not exceed 0.04. For samples 2–6 containing 100% Co, on the other hand, the

values are very similar to those obtained in  $p$ -type filled skutterudites at room temperature ( $ZT \approx 0.2$ ) and suggest that, despite their relatively low electron mobility, these  $n$ -type materials will likely be useful as thermoelectrics as well. In this case the Ce provides substantial phonon scattering without degrading significantly the electron mobility. The existence of two chemically identical compounds which exhibit both  $p$ -type ( $\text{Ce}_y\text{Fe}_{4-x}\text{Co}_x\text{Sb}_{12}$  with  $x < 3$ ) and  $n$ -type ( $\text{Ce}_y\text{Fe}_{4-x}\text{Co}_x\text{Sb}_{12}$  with  $x > 3$ ) behavior is very attractive for

the production of actual thermocouple junctions for power recovery and solid-state cooling applications.

#### ACKNOWLEDGMENTS

The authors are grateful to Chuck Murphy for experimental assistance, Rick Waldo and Noel Potter for microprobe and chemical analysis, respectively, and Dr. David Singh and Dr. Glen Slack for fruitful discussions. This work was supported under ONR Grant No. 0014-96-10181.

- <sup>1</sup>B. C. Sales, D. Mandrus, and R. K. Williams, *Science* **272**, 1325 (1996).
- <sup>2</sup>J.-P. Fleurial, T. Caillat, A. Borshchevsky, D. T. Morelli, and G. P. Meisner, in *Proceedings of the 15th International Conference on Thermoelectrics*, edited by T. Caillat (Institute of Electrical and Electronics Engineers, Piscataway, NJ, 1996), p. 91.
- <sup>3</sup>B. Chen, J.-H. Xu, C. Uher, D. T. Morelli, G. P. Meisner, J.-P. Fleurial, T. Caillat, and A. Borshchevsky, *Phys. Rev. B* **55**, 1476 (1997).
- <sup>4</sup>L. Nördstrom and D. J. Singh, *Phys. Rev. B* **53**, 1103 (1996).
- <sup>5</sup>I. Oftedal, *Z. Kristallogr.* **66**, 517 (1928).
- <sup>6</sup>S. Rundquist and N.-O. Ersson, *Arkiv. För Kemi* **30**, 103 (1968).
- <sup>7</sup>A. Kjekshus and T. Rakke, *Acta Chem. Scand.* **28**, 99 (1974).
- <sup>8</sup>J.-P. Fleurial, T. Caillat, and A. Borshchevsky, in *Proceedings of the 13th International Conference on Thermoelectrics*, edited by B. Mathiprakasham (AIP, New York, 1995), p. 40.
- <sup>9</sup>D. J. Singh and W. E. Pickett, *Phys. Rev. B* **50**, 11 235 (1994).
- <sup>10</sup>D. T. Morelli, T. Caillat, J.-P. Fleurial, J. W. Vandersande, B. Chen, and C. Uher, *Phys. Rev. B* **51**, 9622 (1995).
- <sup>11</sup>A. Borshchevsky, T. Caillat, and J.-P. Fleurial, in *Proceedings of the 15th International Conference on Thermoelectrics*, (Ref. 2), p. 112.
- <sup>12</sup>G. A. Slack and V. G. Tsoukala, *J. Appl. Phys.* **76**, 1665 (1994).
- <sup>13</sup>W. Jeitschko and D. J. Braun, *Acta Crystallogr. Sect. B* **33**, 3401 (1977).
- <sup>14</sup>D. J. Braun and W. Jeitschko, *J. Less-Common Met.* **72**, 147 (1980).
- <sup>15</sup>D. J. Braun and W. Jeitschko, *J. Solid State Chem.* **32**, 357 (1980).
- <sup>16</sup>G. P. Meisner, *Physica B & C* **108B**, 763 (1981).
- <sup>17</sup>G. P. Meisner, M. S. Torikachvili, K. N. Yang, M. B. Maple, and R. P. Guertin, *J. Appl. Phys.* **57**, 3073 (1985).
- <sup>18</sup>D. T. Morelli and G. P. Meisner, *J. Appl. Phys.* **77**, 3777 (1995).
- <sup>19</sup>G. S. Nolas, G. A. Slack, D. T. Morelli, T. M. Tritt, and A. C. Ehrlich, *J. Appl. Phys.* **79**, 4002 (1996).
- <sup>20</sup>J. Ackermann and A. Wold, *J. Phys. Chem. Solids* **38**, 1013 (1977).
- <sup>21</sup>M. E. Danebrock, C. B. H. Evers, and W. Jeitschko, *J. Phys. Chem. Solids* **57**, 381 (1996).
- <sup>22</sup>F. Grandjean, A. Gerald, D. J. Braun, and W. Jeitschko, *J. Phys. Chem. Solids* **45**, 877 (1984).
- <sup>23</sup>T. Caillat, A. Borshchevsky, and J.-P. Fleurial, *J. Appl. Phys.* **80**, 4442 (1996).
- <sup>24</sup>L. D. Dudkin and N. Kh. Abrikosov, *USSR J. Inorg. Chem.* **1**, 169 (1956).
- <sup>25</sup>J. W. Sharp, E. C. Jones, R. K. Williams, P. M. Martin, and B. C. Sales, *J. Appl. Phys.* **78**, 1013 (1995).
- <sup>26</sup>H. J. Goldsmid, *Applications of Thermoelectricity* (Methuen, London, 1960).
- <sup>27</sup>V. Narayanamurti and R. O. Pohl, *Rev. Mod. Phys.* **42**, 201 (1970).
- <sup>28</sup>G. S. Nolas, V. G. Harris, T. M. Tritt, and G.A. Slack, *J. Appl. Phys.* **80**, 6304 (1996).
- <sup>29</sup>T. Caillat, J. Kulleck, A. Borshchevsky, and J.-P. Fleurial, *J. Appl. Phys.* **79**, 8419 (1996).